Nanoscale Advances

ROYAL SOCIETY OF CHEMISTRY

PAPER

View Article Online
View Journal | View Issue



Cite this: *Nanoscale Adv.*, 2024, **6**, 3573

# The *p*-diethanolaminomethylcalix[4]arene-incorporated polyacrylonitrile-based facilitated-transport-nanofiber mat for $O_2/N_2$ separation

Mehwish Ajmal, Saeed Ahmed Memon, Huma Shaikh, * Shahabuddin Memon and Shahnila Shah

Received 8th January 2024
Accepted 21st May 2024

DOI: 10.1039/d4na00019f

rsc.li/nanoscale-advances

Separation of gases from air mixture is one of the most challenging and laborious separations due to the remarkably uniform molecular size of gas molecules. Therefore, the present study aimed to synthesize polyacrylonitrile-based nanofibers mat(NM) impregnated with *p*-diethanolaminomethylcalix[4]arene (PAN/*p*-DEAC4 NM) for the separation of two crucial gases $O_2$ and $N_2$. The affinity of the prepared PAN/*p*-DEAC4 NM for $O_2$ was examined by optimizing the loading concentration of *p*-DEAC4 in the range from 5% to 20% (w/v). The results showed remarkable performance of the PAN/*p*-DEAC4 NM for $O_2/N_2$ separation with a superior $O_2/N_2$ selectivity of 12.75 and excellent permeance of 10.2 GPU for $O_2$ and 0.8 GPU for $N_2$ at 2 bar. The PAN/*p*-DEAC4 NM followed a facilitated transport mechanism for the separation of gases and it was revealed that the *p*-DEAC4 platform in the PAN NM is facilitating the transport of $O_2$ due to its greater affinity towards $O_2$. BET analysis revealed that the prepared NM possesses non-porous morphology with a surface area of 12.69 $m^2\ g^{-1}$. SEM micrographs also confirmed the formation of defect-free NM. Thus, this study presents a unique perspective and direction for fabricating highly permeable nanofiber mats for $O_2/N_2$ separation.



## Introduction

The crucial gases oxygen ($O_2$) and nitrogen ($N_2$) have been used in the medicinal and chemical sectors.[1–3] Importantly, $O_2$ is required in several chemical processes such as gasification of coal,[4] glass manufacture,[5] natural gas combustion,[6] and welding.[7] $N_2$ is used for manufacturing ammonia ($NH_3$),[8] which is used as a coolant in the food industry and for medicinal purposes.[9–11] In terms of medicine, people suffering from respiratory disorders such as severe acute respiratory syndrome (SARS) and COVID-19 require a high level of oxygen.[12,13] Several techniques have been used to separate $O_2/N_2$ gases including polymer-based mixed matrix membranes (MMMs),[14] pressure swipe absorption,[15] and cryogenic distillation.[16] In particular, the membrane technologies are appealing due to their compact footprint, environmentally friendly nature, cheap operating cost, and simplicity of integration with current industrial processes.[17] The membrane technology has greatly emerged after the fabrication of MMMs as they resolved the problems related to polymeric or inorganic membranes.[18,19] MMMs are mostly fabricated by dispersing porous fillers such as metal–organic frameworks (MOFs), carbon nanotubes, graphene derivatives, and zeolites in polymer matrices.[20,21] Recently, a cellulose acetate-based MMM embedded with MgO nanorods (MgO/CA) was prepared using solution casting and a solvent evaporation method. The MMM material was used for the separation of $H_2/CH_4$, $CO_2/CH_4$, and $H_2/CO_2$ gases. MgO/CA membranes loaded with 15% of MgO nanorods produced permeability of 77.80 and 62.90 barrer for $H_2$ and $CO_2$, respectively.[22] In another study, a MMM comprised of porous carbon-based zinc oxide composite (C@ZnO) embedded into a polymer of intrinsic microporosity (PIMs) was reported to possess high permeability due to the presence of sufficient interconnected pores provided by C@ZnO. The C@ZnO/PIM MMM showed permeability of 13 215 barrer for $CO_2$ with $CO_2/N_2$ and $CO_2/CH_4$ selectivity of 21.5 and 14.4, respectively.[23] Herein, it is worth mentioning that the separation of $O_2$ and $N_2$ is very difficult to achieve with high selectivity value due to the minute difference in their kinetic diameters of 3.46 Å and 3.64 Å for $O_2$ and $N_2$, respectively.[24] A MMM based on a polymeric blend of poly(2-acrylamido-2-methyl-1-propanesulfonic acid) and polyvinyl chloride embedded with $Co_3O_4$/GO was evaluated for $O_2/N_2$ separation. The said membrane showed a higher affinity for $O_2$ with $O_2/N_2$ selectivity of 2.58 when 0.05% (w/v) of $Co_3O_4$/GO nanocomposite was loaded.[25] The permeation flux could be improved by using fillers with inherent porosity and affinity. The poor affinity of fillers directs the amount of inorganic fillers and results in aggregation and defective assemblies of the inorganic nanofiller. Recently, fillers modified with organic structures are showing improved phase compatibility and polymer/filler interaction. Therefore, macrocycles are organic

*National Centre of Excellence in Analytical Chemistry, University of Sindh, Jamshoro, 76080, Pakistan. E-mail: huma.hashu@gmail.com; Tel: +92-322-3047472*

compounds that possess cavities and specific binding sites and that can be easily incorporated into MMMs with superior separation efficiency.[26] The calix[*n*]arene family is amongst the macrocycles that form oligomers by incorporating *n* number of phenolic units using methylene linkage. They possess hydrophobic cavities with a prominent 3D structure whose size is directly proportional to the number of phenolic units that form macrocycles.[27] The calix[*n*]arenes are able to complex with ions, biomolecules,[28] neutral molecules, drugs,[29] *etc.* The calix[*n*]arenes are insoluble in water, flexible and versatile in terms of their excellent synthetic strategies and functionalizations.[30] The upper and lower rims of calix[*n*]arenes can be functionalized with a variety of similar and different functional groups.[31] The flexible functionalization of lower and upper rims of calix[*n*]arene allows regulating the conformational mobility of macrocycle and defines the properties of host with respect to the size and shape of the cavity and recognition sites in the macrocycle.[32] Hence, the intrinsic porosity of calixarenes is advantageous when it is used in polymeric membranes for gas separation. The calixarenes based fillers result in additional permeation paths that result in enhanced permeability of the polymeric membrane. Moreover, their recognition ability can increase the selectivity of the membrane exponentially. Here, it is worth mentioning that in comparison to inorganic fillers the organic fillers show more compatibility towards polymeric matrix. Thus, calixarenes are one of the most promising candidates for the development of next-generation membranes.[33] Chapala *et al.*[34] fabricated substituted Calix[4]arene and calix[8]arene based poly(3-trimethylsilyltricyclononene-7) membranes and studied their gas separation properties. Their study revealed that incorporation of calixarenes into the membranes enhanced their selectivity, however, the permeability of the membranes was compromised. The calix[4]arene substituted with ethyl and tert-butyle functionalities based poly(3-trimethylsilyltricyclononene-7) membrane showed a separation factor of 11.4 for the $H_2/N_2$ gas pair, which is more than two times higher than the separation factor offered by neat poly(3-trimethylsilyltricyclononene-7) membrane (separation factor 5.2). While the permeability coefficient of the substituted calixarene-based membrane was reduced to 1000 barrer from 2060 barrer (neat membrane). Calixarenes derivatives have also been explored for the sorption of $CO_2$. A study was carried out to evaluate the $CO_2$ sorption ability of *p-tert*-butylcalix[4]arene incorporated Pebax-1675-based MMM. The calixarene-incorporated MMM showed superior permeability for $CO_2$, *i.e.*, 265.18 barrer and 51.51 barrer in $CO_2/CH_4$ and $CO_2/N_2$ gas pairs, respectively, which was many folds higher than the permeability offered by Pebax-1657 neat membrane when the same gas pairs were separated.[35]

The Permea (Air Products) company produced the first gas-separation membrane gadgets for hydrogen separation in 1980. However, only a few polymeric materials are being used in the development of industrialized gas separation membranes, which is a fairly very small number when compared to the many hundreds of polymer materials that are being prepared and examined for the separation of gases.[36] Some academic and industrial executives criticized the problem of the lack of development in engineering and membrane technology.[37] Most scientists and scholars emphasized inventing innovative polymeric membrane materials with superior selectivity and permeability instead of exploring the process of creating ultra-thin membranes with greater fluxes that fulfill the requirements of industries. As a result, numerous membrane materials with superior selectivity and permeability above the 'Robeson upper limits' have not been available for sale.[38,39] It is because they are (1) too costly, (2) too brittle, (3) insoluble, and (4) non-processable. To achieve a high flux, modern membranes often contain less than 100 nm thickness with a dense selective layer.[40]

In this regard, three-dimensional infrastructure of electrospun nanofibers mat having reasonable porosity and a significant surface area are being employed for gas separation. Electrospun nanofibers have been recently explored for many applications such as fuel cells,[41] drug delivery and wound dressing,[42] tissue engineering[43] electronic applications,[44] catalysis,[45] environmental remediation and filtration.[46–48]

Separation of gases *via* nanofiber-based membranes is an area of interest for academic researchers as well as for industrial sector.[49] Consequently, a new composite membrane composed of defect-free nanofibers was used for gas separation ($CO_2/N_2$). A "reinforced-concrete" framework with good adhesion reliability was produced in the nanofiber composite membranes when PAN nanofibers penetrated into the PEO substrate (NFCM). Additionally, each PEO/PAN NFCMs exhibits a slight decline in the permeability of $CO_2$ as compared to a neat PEO membrane because of the PAN nanofiber's hindrances to the $CO_2$ molecules. Nevertheless, compared to a similar neat PEO membrane, the $CO_2/N_2$ selectivity for every NFCM was determined in the range of 13–15. Findings showed that the $CO_2/N_2$ selectivity of the 3 : 7/PAN NFCM was 65.4, exceeding Robeson's 2008 maximum limit.[50] The cellulose nanofiber-based ZIF-8 (CNF@ZIF-8) was fabricated using suction filtration and crystal formation of ZIF-8 on CNFs. The implicit selectivity of ZIF-8 succeeded in the separation of gases as the ZIF-8 dosage was raised to a sufficient level. According to the results, at 25 °C and 0.3 MPa, (CNF@ZIF-8-70) showed the best separation performance; the $CO_2$ permeance was observed as 550 barr with excellent $CO_2/CH_4$ and $CO_2/N_2$ selectivities of 36.2 and 45.5, respectively.[51] Nevertheless, the electrospun fibers mentioned above have some drawbacks, including lower chemical and mechanical stability and lesser adsorption selectivity. Therefore, calixarenes-based nanofiber membranes are a versatile choice to overcome these issues. It is an organic compound that possesses pores up to sub-nano-meters because of multiple benzene rings in its structure.[52] Calixarenes are well recognized for their air filtration, sorption selectivity and diverse applications. They are commonly used in host-guest chemistry due to their limitless derivative prospects driven by their unusual 3D structure and propensity to produce multiplexes with metal ions.[53,54] Substituted calix[*n*]arene integration in layers of nanofibrous membranes benefits water/ethanol separation.[52] Calixarenes have been explored for their characteristics at the

 

nanoscale by impregnating them within polymers to produce mixed matrix electrospun nanofibers.[55–57]

The addition of calixarene as a filler in a nanofibrous membrane can increase its separation efficiency for the mixture of gases.[58] Therefore, owing to the diversity in the nature of calixarenes, the current study aimed to prepare polyacrylonitrile NM impregnated with *p*-diethanolaminomethylcalix[4]arene (PAN/*p*-DEAC4 NM) using the electrospinning technique. Several sophisticated analytical techniques were used to characterize the prepared materials. Finally, the synthesized NMs were applied for the separation of $O_2/N_2$ gases. The gas separation experiments revealed excellent $O_2/N_2$ selectivity of PAN/*p*-DEAC4 NM that is 12.75 at a pressure of 2 bar with extraordinary permeance of 10.2 and 0.80 GPU for $O_2$ and $N_2$, respectively.

## Experimental section

### Materials and reagents

All the chemicals utilized for the synthesis and the preparation of solutions were of analytical grade. Chemicals such as polyacrylonitrile (MW 150 000), diethanolamine, *p*-*tert*-butyl phenol, formaldehyde, sodium hydroxide and aluminum trichloride anhydrous were acquired from Sigma Aldrich (USA). Solvents such as *N*,*N*-dimethylformamide (DMF), methanol, toluene, tetrahydrofuran (THF), glacial acetic acid, diphenyl ether and ethyl acetate were obtained from Merck (Germany). A thin layer Chromatography (TLC) study was carried out on percolated silica gel sheets from Merck (Germany).

### Instrumentation

A (Galzlenkamp, England) equipment was used to determine the melting point in a sealed capillary. To prepare NM, an electrospinning and electrospraying system (Qosain Scientific HBY30, Lahore, Pakistan) with a superior voltage power supply as an electric field was used. A (Thermo Nicollet AVATAR 5700) spectrometer was used to obtain ATR-FTIR spectra with a spectral range of 4000–400 $cm^{-1}$. The morphology of NM was explored using SEM (A JSM-6380) technique.

### Synthesis

Scheme 1 represents the entire synthesis of *p*-*tert*-butylcalix[4]arene (**1**), calix[4]arene (**2**) and *p*-diethanolaminomethylcalix[4]arene (*p*-DEAC4). These all compounds were prepared following the reported methods.[59–61]

### Electrospinning

The mixture of PAN (12% w/v) and *p*-DEAC4 (5–25% w/v) was prepared in DMF. The components of the mixture were stirred under ambient conditions for 4 h in order to ensure sufficient blending. Finally, the well-blended mixture was filled in a 10 mL syringe having a flat-tip stainless steel needle with a 0.7 mm internal diameter. NM was obtained on a stationary collector (aluminum foil as a collection screen). A voltage of 12 kV was applied between the accumulator and the needle tip with a distance of 12 cm between them. During electrospinning, temperature and humidity were maintained at 25 °C and 50%, respectively.[62]

### Gas permeation studies

The permeation studies were carried out using aluminum stainless steel permeation gas equipment with an optimal area of 8 $cm^2$.[63] Both $O_2$ and $N_2$ gas flow rates were measured using a bubble flow meter at fixed temperature and different pressures ranging from 1 to 4 bars. The following equation was used to calculate the permeability of the membrane.

$$P = \frac{QL}{\Delta PA}$$

where $Q$, $\Delta P$, $A$ and $L$ indicate the flow rate (mL $min^{-1}$), change in permeate pressure and feed pressure (bar), area of the membrane ($m^2$) and thickness of the membrane (m). However,

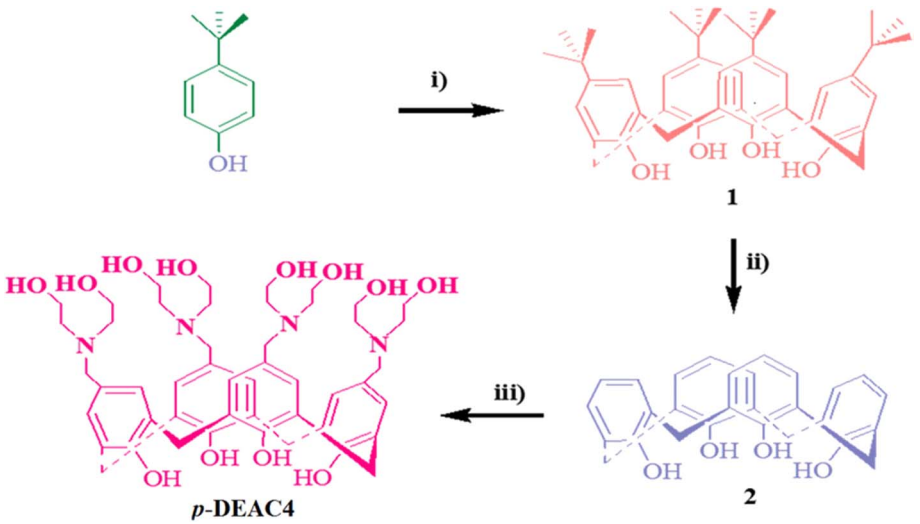


Scheme 1 Synthesis of calix[4]arene derivatives (i) HCHO/NaOH, (ii) $AlCl_3$/phenol, and (iii) diethanolamino/THF/HCHO/acetic acid.

the following equation was used to calculate the selectivity of the membrane $\alpha_{O_2/N_2}$ for $O_2$ and $N_2$.

$$\alpha_{O_2/N_2} = \frac{P_{O_2}}{P_{N_2}}$$

## Results and discussion

### Characterization

**ATR-FTIR study.** Both PAN and PAN/*p*-DEAC4 NM were studied simultaneously employing an interfacial technique of ATR-FTIR spectroscopy to confirm the integration of calixarene units into the NM. The spectra (a) PAN NM and (b) PAN/*p*-DEAC4 NM are presented in Fig. 1. The spectrum Fig. 1a belongs to PAN NM without calix[4]arene. The stretching vibrations found at 2920–2950 $cm^{-1}$ corresponded to CH and $CH_2$ groups, while the strong peak at 2242 $cm^{-1}$ represented the deformation vibration of the CN functional group. The deformation vibrations in the range of 1250–1453 $cm^{-1}$ are produced by $CH/CH_2$ functionalities of PAN NM.[64,65] However, the spectrum (b) shows the appearance of characteristic bands of PAN/*p*-DEAC4 at 3486, 3025, 2925, 1601, and 1492 $cm^{-1}$. The spectrum further indicates the absence of O–H, the C–H aliphatic stretchings. The appearance of peaks due to the calixarene derivative in PAN/*p*-DEAC4 confirmed the successful attachment of the calixarene derivative at PAN NM.

**SEM study.** The exterior morphologies of PAN and PAN/*p*-DEAC4 NM are presented in Fig. 2. It is evident from Fig. 2 that PAN NMs (Fig. 2a and b) are thinner as compared to PAN/*p*-DEAC4 (Fig. 2c and d). This is because of the lower viscosity of the PAN solution due to the absence of *p*-DEAC4. The cross-sectional morphology of the SEM images shows that there was no phase separation, and both nanofibers are comparable. SEM images further confirmed that PAN NM is homogeneous with and without *p*-DEAC4 and the presence of *p*-DEAC4 did not affect the homogeneity of PAN NM. This also revealed that *p*-DEAC4 was evenly distributed into the matrix of nanofibers. However, the diameter of PAN/*p*-DEAC4 NM was slightly greater compared to that of PAN NM because of its higher solution viscosity due to the existence of *p*-DEAC4 molecules. Hence, the exterior morphology of PAN/*p*-DEAC4 NM is obviously different from that of PAN NM, as evidenced in the SEM images.[66]

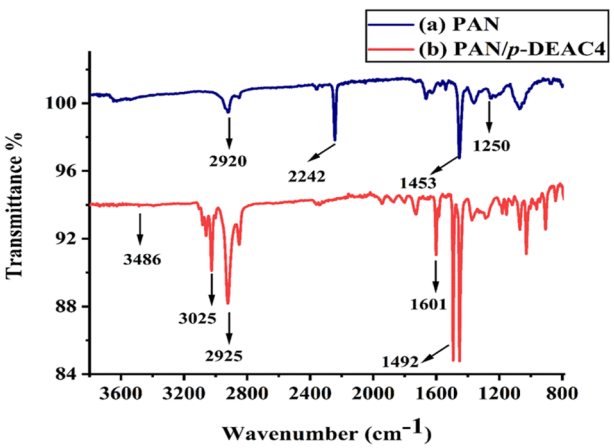


Fig. 1 ATR-FTIR spectra of (a) PAN and (b) PAN/*p*-DEAC4 NM.

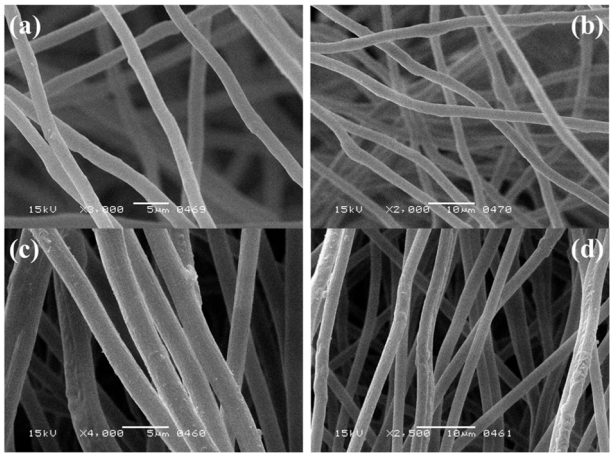


Fig. 2 SEM micrographs of (a and b) PAN and (c and d) PAN/*p*-DEAC4 NM.

**BET analysis.** $N_2$ adsorption–desorption studies were performed to analyze the specific surface area and porosity of the produced PAN/*p*-DEAC4 NM, and the findings are shown in Fig. 3a and b. The isotherms in Fig. 3a revealed type II with H3-type hysteresis loop in the relative pressure ranges of 0.025–0.99 with a surface area of 12.69 $m^2\ g^{-1}$, which is typical of the nonporous architectures of PAN/*p*-DEAC4 NM. Overall, the Barrett–Joyner–Halenda (BJH) model was used to calculate the pore diameter and volume, as shown in Fig. 3b. The acquired results are consistent with the previously published literature.[66] The pore diameter and volume were determined to be 4.18 nm and 0.07 cc $g^{-1}$, respectively.

### Gas permeation results

Analyses of gas permeation studies using PAN and PAN/*p*-DEAC4 NMs of various concentrations (5–20% w/v *p*-DEAC4) were conducted. The influence of the flow rate and loading amount of *p*-DEAC4 on the permeability and separation factor of PAN/*p*-DEAC4 NM for $O_2/N_2$ separation were examined by varying the pressure from 1 bar to 4 bar. Fig. 4a shows that the permeance of PAN NM for $O_2$ is high at a pressure of 1 bar and it gradually decreases with increasing pressure from 1 bar to 4 bar. The permeance of PAN/*p*-DEAC4 NMs decreases with increasing percent of *p*-DEAC4 at a pressure of 1 bar. The 5% and 10% PAN/*p*-DEAC4 NM showed consistent results at pressures of 1 bar and 2 bar but the permeance of all fibers decreased at pressures of 3 and 4 bar due to the short interaction time of $O_2$ with NMs. The extremely high permeance of PAN NM is because the fibrous texture of mats holds huge voids between the nanofibers and gas can pass through those voids very quickly without interacting with nanofibers. PAN/*p*-DEAC4 NMs showed a similar trend of permeance for $N_2$ (Fig. 4b). However, their overall permeance for $N_2$ was less than the permeance of $O_2$. The selectivity results of

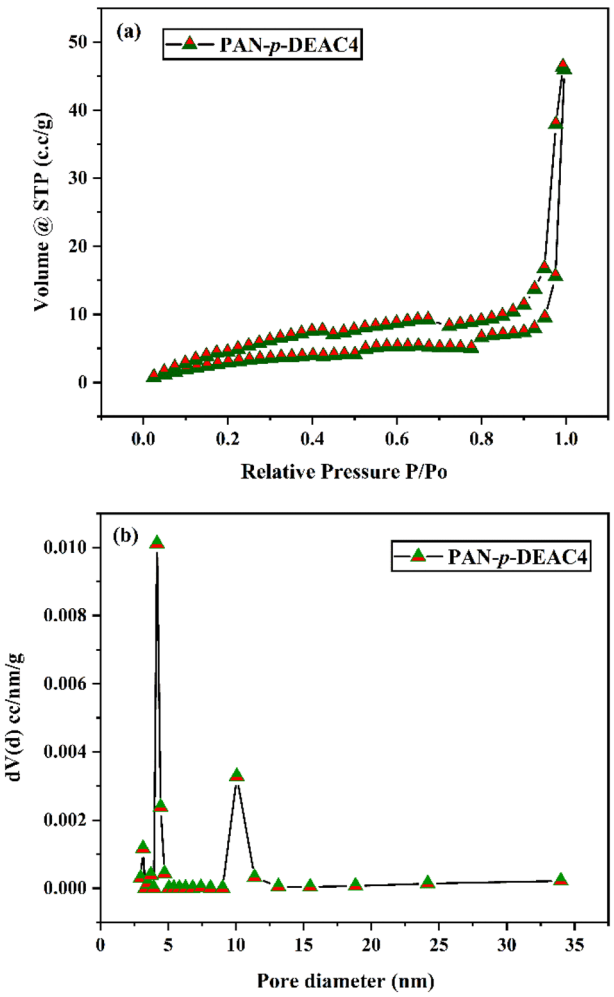


Fig. 3 (a) $N_2$ adsorption and desorption isotherms and (b) BJH pore-size distributions of PAN/*p*-DEAC4 NM.

PAN/*p*-DEAC4 NM showed that the presence of *p*-DEAC4 is converting PAN/*p*-DEAC4 NM into facilitated transport mats. The PAN/*p*-DEAC4 NM were highly selective for $O_2$ at a pressure of 2 bar and revealed the $O_2/N_2$ selectivity in the range of 3.33 to 12.75 when loaded with *p*-DEAC4 in the range of 5 to 20% (Fig. 4c). The selectivity of PAN/*p*-DEAC4 increased with increasing concentration of *p*-DEAC4 which reveals the successful interaction of $O_2$ with *p*-DEAC4 into PAN/*p*-DEAC4. In comparison to PAN/*p*-DEAC4 NM; the PAN NM showed an $O_2/N_2$ selectivity of 1.4, which is many folds less than the selectivity of PAN/*p*-DEAC4 NM membranes.[67] The outcomes further revealed that the permeance of $O_2$ is higher as compared to that of $N_2$ across all membrane samples at all pressures. This phenomenon is primarily owing to the smaller kinetic diameter of $O_2$ as compared to that of $N_2$ along with the facilitated transport of $O_2$ by PAN/*p*-DEAC4 NM, which speeds up the propagation of $O_2$ molecules while expanding the separation factor over $N_2$ molecules.[67] The results also revealed that nanofiber-based mats showed good permeance at lower pressures and overall permeance is reduced at pressure of 3 and 4 bars. It may be due to the fact that NMs are comprised of layers of nanofiber

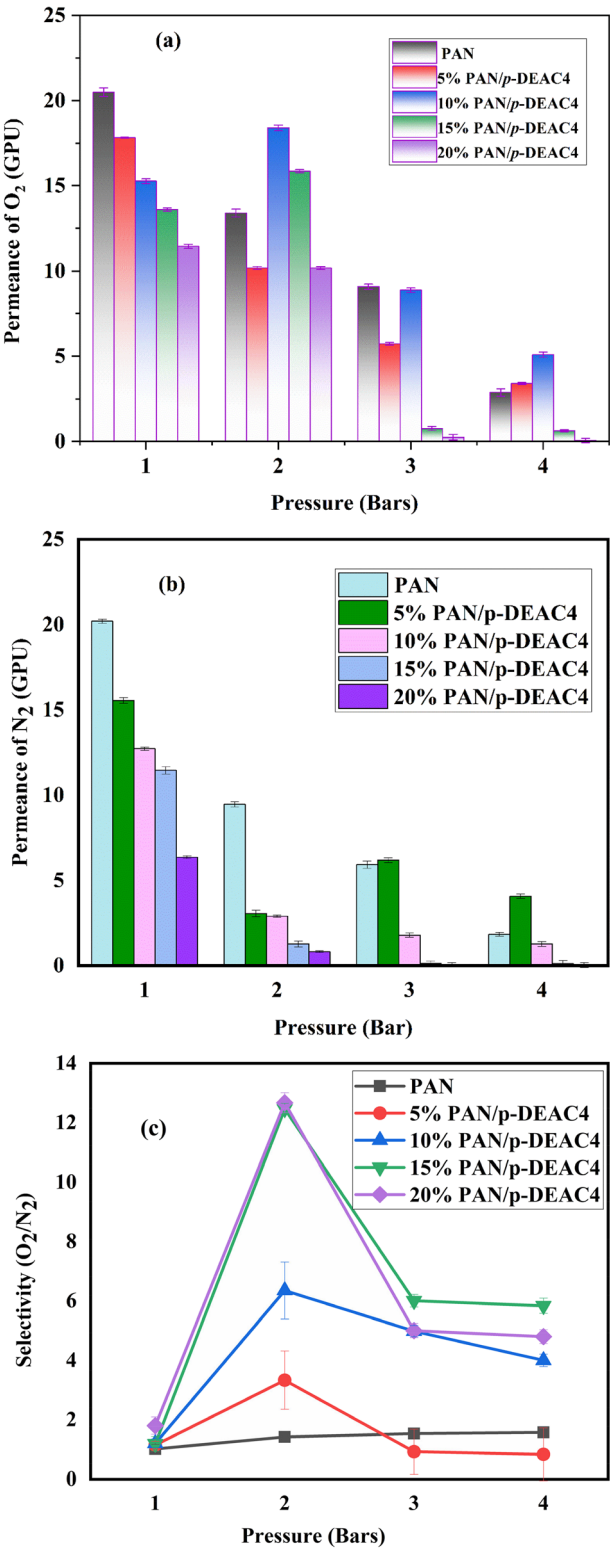


Fig. 4 Permeance of different membranes under study for (a) $O_2$ (b) $N_2$ and (c) selectivity at various pressures in the range of 1–4 bars.

membranes and when the pressure increases, the gas molecules intercalate into the layers of membranes and produce back pressure that hinders the fast flow of gas. Pu-PTH-based polymer membranes embedded using $TiO_2$ and $SiO_2$ nanoparticles were

Table 1 Gas permeation analysis results obtained at different concentrations of *p*-DEAC4 in PAN/*p*-DEAC4 NM

| Samples | Pressure (bar) | Permeance (GPU) | | Selectivity |
|---|---|---|---|---|
| | | $P(O_2)$ | $P(N_2)$ | $O_2/N_2$ |
| PAN NM | 1 | 20.5 ± 0.25 | 20.2 ± 0.12 | 1.0 ± 0.15 |
| | 2 | 13.4 ± 0.23 | 9.45 ± 0.15 | 1.4 ± 0.19 |
| | 3 | 9.1 ± 0.15 | 5.92 ± 0.21 | 1.5 ± 0.18 |
| | 4 | 2.9 ± 0.21 | 1.83 ± 0.11 | 1.6 ± 0.16 |
| PAN/*p*-DEAC4 NM (5% w/v) | 1 | 17.8 ± 0.03 | 15.54 ± 0.16 | 1.14 ± 0.12 |
| | 2 | 10.2 ± 0.09 | 3.05 ± 0.19 | 3.3 ± 0.98 |
| | 3 | 5.7 ± 0.07 | 6.2 ± 0.15 | 0.92 ± 0.76 |
| | 4 | 3.4 ± 0.05 | 4.1 ± 0.12 | 0.8 ± 0.89 |
| PAN/*p*-DEAC4 NM (10% w/v) | 1 | 15.3 ± 0.14 | 12.7 ± 0.09 | 1.2 ± 0.15 |
| | 2 | 18.4 ± 0.17 | 2.9 ± 0.07 | 6.3 ± 0.96 |
| | 3 | 8.9 ± 0.13 | 1.8 ± 0.12 | 4.98 ± 0.19 |
| | 4 | 5.1 ± 0.15 | 1.3 ± 0.14 | 4 ± 0.21 |
| PAN/*p*-DEAC4 NM (15% w/v) | 1 | 13.6 ± 0.09 | 11.45 ± 0.21 | 1.2 ± 0.25 |
| | 2 | 15.8 ± 0.08 | 1.3 ± 0.18 | 12.46 ± 0.19 |
| | 3 | 0.76 ± 0.12 | 0.13 ± 0.15 | 6 ± 0.21 |
| | 4 | 0.63 ± 0.06 | 0.11 ± 0.19 | 5.8 ± 0.25 |
| PAN/*p*-DEAC4 NM (20% w/v) | 1 | 11.45 ± 0.12 | 6.4 ± 0.08 | 1.8 ± 0.29 |
| | 2 | 10.2 ± 0.08 | 0.8 ± 0.05 | 12.75 ± 0.34 |
| | 3 | 0.25 ± 0.16 | 0.05 ± 0.12 | 5 ± 0.24 |
| | 4 | 0.06 ± 0.13 | 0.013 ± 0.14 | 4.8 ± 0.23 |

reported by Azari Monsefi M and his colleagues for the separation of $O_2$ and $N_2$. After 20% loading of the filler, these membranes produced 10 barrer permeability for $O_2$ and a separation factor of 2.5.[68] A mixed matrix membrane based on Pebax-1657 incorporated with $BaFe_{12}O_{19}$ nano-particles was introduced by Nikpour N. *et al.* for the separation of $O_2/N_2$. The resulting membrane showed the $O_2/N_2$ gas selectivity of 4.2 with $O_2$ gas permeability of 12.2 (barrer).[69] A membrane of poly(ether block amide) and PSF polymeric material for the enrichment of oxygen was introduced that showed the $O_2/N_2$ gas selectivity of 3.71 with a permeance of 39.81 GPU at 5 bar pressure.[70] Mohammad R. M *et al.* presented a study in which a multi-layer composite membrane composed of PSF/polyester was used for the separation of $O_2/N_2$ that showed selectivity of 5.92 and $O_2$ permeance of 0.7104 (GPU).[71] Further research has been published on the usefulness of PDMS polymeric membrane incorporated with carbon nanotubes (CNTs) for separation of $O_2$ and $N_2$, the selectivity of 2.69 was obtained in this study at 32.25 barrer.[72]

In contrast, the present study reveals that PAN/*p*-DEAC4 NM membranes have a tremendous permeance of 10.2 GPU for $O_2$ at low pressures. As the concentration of *p*-DEAC4 was raised from 5% to 20%, the separation factor of membranes for $O_2$ was increased (Fig. 4c and Table 1). This phenomenon is caused by PAN/*p*-DEAC4 NM; the amended linkages of calixarene moiety with $O_2$ eventually served by facilitating the transport of excess $O_2$ across the membranes.[73]

The maximum selectivity of $O_2/N_2$ was found to be 12.75 when 20% (w/v) of the *p*-DEAC4 was loaded with PAN NM at 2

Table 2 Comparison of permeability and selectivity of PAN/*p*-DEAC4 NM with recently reported MMMs

| S. No. | Materials | Fillers | Permeability $P(O_2)$ barrer | Permeability $P(N_2)$ barrer | $\alpha_{(O_2)/(N_2)}$ | Ref. |
|---|---|---|---|---|---|---|
| 1 | Poly(aryl ether sulfone) (PES) | — | 1.48 | 0.14 | 10.6 | 74 |
| 2 | Pebax | $Fe_3O_4$@ZIF-8 | 194 | 20 | 11.97 | 76 |
| 3 | Matrimid | f-MWCNT | 2.87 | — | 7.83 | 77 |
| 4 | Polyimide | Cerium oxide ($CeO_2$) | 240.3 | 14.7 | 16.3 | 78 |
| 5 | Sulfonated poly(ether ether ketone) (sPEEK) and poly(etherimide) (PEI) (80/20) | MWCNT | 15.245 | 11.985 | 1.272 | 79 |
| 6 | Polymer of intrinsic microporosity (PIM-1) | ZIF-8-7 | 1287 | 351 | 3.7 | 80 |
| 7 | PIM-1 | Cobalt-based ionic liquid@polyarylate (core–shell) composite nanospheres CILs@PAR (c–s) CNPs | 140 | 32 | 5 | 81 |
| 8 | PAN | *p*-DEAC4 | 1428 | 112 | 12.75 | Present work |

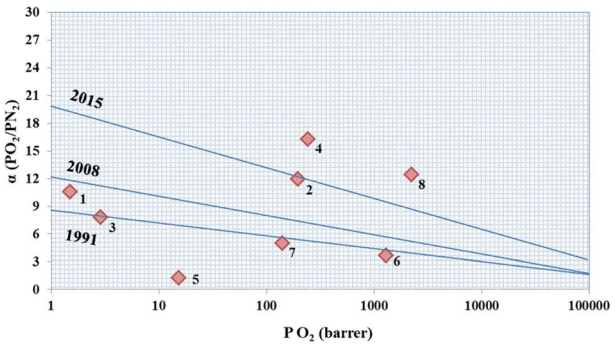


Fig. 5 Robeson's 1991, 2008 and Pinnau's upper bound curves for $O_2/N_2$ permeation and selectivity through MMMs presented in Table 2.

bar having the best permeance of 10.2 GPU for $O_2$. The above findings further demonstrated the cost-effectiveness of the synthesized PAN/*p*-DEAC4 NM, as excellent outcomes were achieved at a pressure of 2 bar. Nevertheless, a concentration lower than 20% also worked and produced far better permeance and $O_2/N_2$ selectivity when compared to polymeric or mixed matrix membranes.

### Comparison of PAN/*p*-DEAC4 NM with recently reported MMM

The performance of PAN/*p*-DEAC4 NM was compared with those of the recently reported membranes for the separation of $O_2/N_2$ (Table 2). It can be observed that most of the MMMs have inorganic fillers with the exception of a membrane composed of neat PES.[74] The said membrane showed an excellent selectivity of 10.6 with greatly compromised permeability for both $O_2$ and $N_2$ (Table 2), and therefore, falls under Robeson's upper bound limit given in 2008 (Fig. 5). Robeson explained the trade-off phenomenon between the permselectivity and permeability of membranes for gases. He created the first upper bound curve in 1991[39] that was further updated in 2008[38] and later in 2015 by Pinnau's[75] (Fig. 5). It can be observed that most of the recently reported membranes could not cross the upper bound line of even 2008. Very limited numbers of membranes are able to achieve a higher trade-off between permselectivity and permeability, which is an ultimate industrial requirement. PAN/*p*-DEAC4 NM is one of the very few MMMs that are able to cross the upper bound line of 2015 that reveals the excellent permselectivity of PAN/*p*-DEAC4 NM without compromising its permeability for $O_2$. Moreover, PAN/*p*-DEAC4 NM proved itself as cost effective alternative for the separation of $O_2/N_2$ by producing excellent separation performance at pressure of 2 bars.

## Conclusion

In this research work, PAN/*p*-DEAC4 NM was fabricated by electrospinning technique. The PAN/*p*-DEAC4 NM was characterized by various sophisticated analytical techniques. The successfully synthesized PAN/*p*-DEAC4 NM was applied for the separation of $O_2/N_2$ gases. The affinity of the prepared PAN/*p*-DEAC4 NM was examined by optimizing the concentration of *p*-DEAC4, *i.e.*, 5%, 10%, 15% and 20% (w/v) for the separation of the gas pairs $O_2/N_2$. The results showed tremendous performance for $O_2/N_2$ separation with superior $O_2/N_2$ selectivity of 12.75 and excellent permeance. The PAN/*p*-DEAC4 NM followed a facilitated transport mechanism for $O_2/N_2$ separation, which is why, despite of minute difference between the molecular sizes of $O_2$ and $N_2$, very good selectivity for $O_2$ was achieved at 2 bar. Therefore, PAN/*p*-DEAC4 NM is a promising inexpensive membrane for the separation of gas pairs $O_2/N_2$. This study provides a novel perspective and direction for industry to fabricate extremely permeable membranes for the separation and enrichment of $O_2$ and $N_2$.

## Conflicts of interest

All the authors declare that there is no conflict of interest regarding the research work presented in this manuscript.

## Acknowledgements

This work was supported and funded by the Higher Education Commission under project number 9322/Sindh/NRPU/R&D/HEC/.

## References

1 Y. Tang, X. Wang, Y. Wen, X. Zhou and Z. Li, *Ind. Eng. Chem. Res.*, 2020, **59**, 6219–6225.
2 J. Dou, E. Krzystowczyk, X. Wang, A. R. Richard, T. Robbins and F. Li, *J. Phys.: Energy*, 2020, **2**, 025007.
3 M. W. Ackley, *Adsorption*, 2019, **25**, 1437–1474.
4 Y. Wang, P. Niu and H. Zhao, *Fuel Process. Technol.*, 2019, **192**, 75–86.
5 N. I. Min'ko and I. M. Binaliev, *Glass Ceram.*, 2013, **69**, 361–365.
6 V. P. Timón, G. Corchero and J. L. Montañés, *Energy Fuels*, 2017, **31**, 11348–11361.
7 S. P. Lu, H. Fujii, K. Nogi and T. Sato, *Sci. Technol. Weld. Joining*, 2007, **12**, 689–695.
8 D. Wang, L. M. Azofra, M. Harb, L. Cavallo, X. Zhang, B. H. R. Suryanto and D. R. MacFarlane, *ChemSusChem*, 2018, **11**, 3416–3422.
9 M. S. Latifi, G. Colangelo and G. Starace, *Experimental and Computational Multiphase Flow*, 2020, **2**, 109–114.
10 M. T. Masatcioglu and F. Koksel, *J. Sci. Food Agric.*, 2019, **99**, 6796–6805.
11 P. Munsch-Alatossava, R. Käkelä, D. Ibarra, M. Youbi-Idrissi and T. Alatossava, *Front. Microbiol.*, 2018, **9**, 1307.
12 R. Kapoor, J. S. Welsh, V. Dhawan, S. A. Javadinia, E. J. Calabrese and G. Dhawan, *Arch. Toxicol.*, 2021, **95**, 3425–3432.
13 J. T. Schiffer, C. Johnston, A. Wald and L. Corey, *Open Forum Infect. Dis.*, 2020, **7**, ofaa232.
14 S. J. Miller, W. J. Koros and D. Q. Vu, in *Studies in Surface Science and Catalysis*, ed. R. Xu, Z. Gao, J. Chen and W. Yan, Elsevier, 2007, vol. 170, pp. 1590–1596.

15 A. Klimkowicz, T. Hashizume, K. Cichy, S. Tamura, K. Świerczek, A. Takasaki, T. Motohashi and B. Dabrowski, *J. Mater. Sci.*, 2020, **55**, 15653–15666.
16 K. C. Chong, S. O. Lai, H. S. Thiam and W. J. Lau, *Key Eng. Mater.*, 2016, **701**, 255–259.
17 Y. Xiao, B. T. Low, S. S. Hosseini, T. S. Chung and D. R. Paul, *Prog. Polym. Sci.*, 2009, **34**, 561–580.
18 A. Jain, M. Z. Ahmad, A. Linkès, V. Martin-Gil, R. Castro-Muñoz, P. Izak, Z. Sofer, W. Hintz and V. Fila, *Nanomaterials*, 2021, **11**, 668.
19 L. T. Yogarathinam, P. S. Goh, A. F. Ismail, A. Gangasalam, N. A. Ahmad, A. Samavati, S. C. Mamah, M. N. Zainol Abidin, B. C. Ng and B. Gopal, *Chemosphere*, 2022, **293**, 133561.
20 Y. Shen, H. Wang, X. Zhang and Y. Zhang, *ACS Appl. Mater. Interfaces*, 2016, **8**, 23371–23378.
21 Z. Lin, Z. Yuan, Z. Dai, L. Shao, M. S. Eisen and X. He, *Chem. Eng. J.*, 2023, **475**, 146075.
22 M. M. Rajpure, R. B. Mujmule, U. Kim and H. Kim, *Int. J. Hydrogen Energy*, 2024, **50**, 615–628.
23 M. Chen, J. Zhou, J. Ma, W. Zheng, G. Dong, X. Li, Z. Tian, Y. Zhang, J. Wang and Y. Wang, *Green Energy Environ.*, 2024, DOI: **10.1016/j.gee.2024.03.002**.
24 S. Shah, H. Shaikh, S. Hafeez and M. I. Malik, *Pak. J. Anal. Environ. Chem.*, 2020, **21**, 44–53.
25 S. Shah, H. Shaikh, S. Farrukh, M. I. Malik, Z. u. N. Mughal and S. Bhagat, *RSC Adv.*, 2021, **11**, 19647–19655.
26 T. Huang, M. Alyami, N. M. Kashab and S. P. Nunes, *J. Mater. Chem. A*, 2021, **9**, 18102–18128.
27 E. S. Español and M. M. Villamil, *Biomolecules*, 2019, **9**(3), 90.
28 P. B. Crowley, *Acc. Chem. Res.*, 2022, **55**, 2019–2032.
29 Y. Zhou, H. Li and Y.-W. Yang, *Chin. Chem. Lett.*, 2015, **26**, 825–828.
30 Z. Asfari, V. Böhmer, J. Harrowfield, J. Vicens and M. Saadioui, *Calixarenes 2001*, Springer Dordrecht, 1st edn, 2001.
31 S. Viola, G. M. L. Consoli, S. Merlo, F. Drago, M. A. Sortino and C. Geraci, *J. Neurochem.*, 2008, **107**, 1047–1055.
32 M. Malinska, *IUCrJ*, 2022, **9**, 55–64.
33 T.-S. Chung and J.-Y. Lai, *Chem. Eng. Res. Des.*, 2022, **183**, 538–545.
34 P. P. Chapala, M. V. Bermeshev, L. E. Starannikova, V. P. Shantarovich, N. N. Gavrilova, V. G. Avakyan, M. P. Filatova, Y. P. Yampolskii and E. S. Finkelshtein, *J. Membr. Sci.*, 2015, **474**, 83–91.
35 A. Nadeali, M. Zamani Pedram, M. Omidkhah and M. Yarmohammadi, *ACS Sustain. Chem. Eng.*, 2019, **7**, 19015–19026.
36 R. Baker, *Membr. Technol.*, 2001, **2001**, 5–10.
37 R. W. Baker, *J. Membr. Sci.*, 2010, **362**, 134–136.
38 L. M. Robeson, *J. Membr. Sci.*, 2008, **320**, 390–400.
39 L. M. Robeson, *J. Membr. Sci.*, 1991, **62**, 165–185.
40 S. Loeb, The Loeb-Sourirajan membrane: How it came about, in *Synthetic Membranes*, American Chemical Society, 1981, vol. 153, ch. 1, pp. 1–9.
41 S. Yu, S. Xu, R. Khan, H. Zhao and C. Li, *Catal. Sci. Technol.*, 2024, **14**, 820–834.
42 N. Angel, S. Li and L. Kong, *J. Future Foods*, 2024, **4**, 289–299.
43 M. Zhang, S. Xu, R. Wang, Y. Che, C. Han, W. Feng, C. Wang and W. Zhao, *J. Mater. Sci. Technol.*, 2023, **162**, 157–178.
44 V. K. Sharma, G. Chakraborty, S. Narendren and V. Katiyar, *Mater. Adv.*, 2023, **4**, 6294–6303.
45 P. K. Panda, B. Sahoo and S. Ramakrishna, *Int. J. Hydrogen Energy*, 2023, **48**, 37193–37208.
46 D. Pathak, A. Sharma, D. P. Sharma and V. Kumar, *Appl. Surf. Sci. Adv.*, 2023, **18**, 100471.
47 X. Zhang, Z. Ru, Y. Sun, M. Zhang, J. Wang, M. Ge, H. Liu, S. Wu, C. Cao, X. Ren, J. Mi and Y. Feng, *J. Cleaner Prod.*, 2022, **378**, 134567.
48 F. Zhang, Y. Si, J. Yu and B. Ding, *Chem. Eng. J.*, 2023, **456**, 140989.
49 S. L. Regen, *Langmuir*, 2022, **38**, 4490–4493.
50 T. Sun, W. Zheng, J. Chen, Y. Dai, X. Li, X. Ruan, X. Yan and G. He, *J. Membr. Sci.*, 2021, **639**, 119749.
51 M. Jia, X.-F. Zhang, Y. Feng, Y. Zhou and J. Yao, *J. Membr. Sci.*, 2020, **595**, 117579.
52 Y. Ji, S. Dong, Y. Huang, C. Yue, H. Zhu, D. Wu and J. Zhao, *Membranes*, 2024, **14**, 32.
53 X. Hu, Y. Li, Y. Wang, X. Li, H. Li, X. Liu and P. Zhang, *Desalination*, 2010, **259**, 76–83.
54 J. Konczyk, A. Nowik-Zajac and C. A. Kozlowski, *Sep. Sci. Technol.*, 2016, **51**, 2394–2410.
55 M. Chen, C. Wang, W. Fang, J. Wang, W. Zhang, G. Jin and G. Diao, *Langmuir*, 2013, **29**, 11858–11867.
56 S. Koçyiğit, M. Tabakci and İ. Özaytekin, *Polym.-Plast. Technol. Eng.*, 2013, **52**, 141–144.
57 F. Özcan, M. Bayrakcı and Ş. Ertul, *J. Inclusion Phenom. Macrocyclic Chem.*, 2016, **85**, 49–58.
58 P. Chapala, M. Bermeshev, L. Starannikova, V. Shantarovich, N. Gavrilova, V. Avakyan, M. Filatova, Y. P. Yampolskii and E. S. Finkelshtein, *J. Membr. Sci.*, 2015, **474**, 83–91.
59 C. D. Gutsche and K. C. Nam, *J. Am. Chem. Soc.*, 1988, **110**, 6153–6162.
60 C. D. Gutsche and L.-G. Lin, *Tetrahedron*, 1986, **42**, 1633–1640.
61 C. D. Gutsche, M. Iqbal and D. Stewart, *J. Org. Chem.*, 1986, **51**, 742–745.
62 S. Hafeez, X. Fan, A. Hussain and C. F. Martín, *J. Environ. Sci.s*, 2015, **35**, 163–171.
63 S. Hafeez, X. Fan, A. Hussain and C. F. Martín, *J. Environ. Sci.*, 2015, **35**, 163–171.
64 Y. Liu, G. Jiang, L. Li, H. Chen, Q. Huang, T. Jiang, X. Du and W. Chen, *J. Mater. Sci.*, 2015, **50**, 8120–8127.
65 H. Chen, G. Jiang, W. Yu, D. Liu, Y. Liu, L. Li, Q. Huang, Z. Tong and W. Chen, *Powder Technol.*, 2016, **298**, 1–8.
66 S. A. Memon, H. Shaikh, S. Memon, F. K. Mahar and Z. Khatri, *React. Funct. Polym.*, 2022, **175**, 105280.
67 W. Choi, P. G. Ingole, H. Li, S. Y. Park, J. H. Kim, H.-K. Lee and I.-H. Baek, *Microchem. J.*, 2017, **132**, 36–42.
68 M. Azari, M. Sadeghi, M. Aroon and T. Matsuura, *J. Membr. Sci. Res.*, 2019, **5**, 33–43.
69 J. Han, L. Bai, B. Yang, Y. Bai, S. Luo, S. Zeng, H. Gao, Y. Nie, X. Ji and S. Zhang, *Membranes*, 2019, **9**, 115.

70 K. C. Chong, Y. Y. Chan, W. J. Lau, S. O. Lai, A. F. Ismail and H. S. Thiam, *Mal. J. Fund. Appl. Sci.*, 2019, **15**, 50–53.
71 M. R. Moradi, M. P. Chenar, S. H. Noie, M. Hesampour and M. Mänttäri, *Polym. Test.*, 2017, **63**, 101–109.
72 S. Kim, T. W. Pechar and E. Marand, *Desalination*, 2006, **192**, 330–339.
73 J. R. Potts, D. R. Dreyer, C. W. Bielawski and R. S. Ruoff, *Polymer*, 2011, **52**, 5–25.
74 Z. Cheng, P. Wang, Y. Sun, Z. Wang and G. Zhou, *Polymer*, 2024, **297**, 126867.
75 X. Ma, H. W. H. Lai, Y. Wang, A. Alhazmi, Y. Xia and I. Pinnau, *ACS Macro Lett.*, 2020, **9**, 680–685.
76 X. Cao, R. Song, L. Zhang, F. Cheng and Z. Wang, *J. Membr. Sci.*, 2024, **698**, 122624.
77 M. Patil, S. G. Hunasikai, S. N. Mathad, A. Y. Patil, C. G. Hegde, M. A. Sudeept, M. K. Amshumali, A. M. Elgorban, S. Wang, L. S. Wong and A. Syed, *Heliyon*, 2023, **9**, e21992.
78 Z. Gao, B. Zhang, C. Yang and Y. Wu, *Appl. Surf. Sci.*, 2024, **649**, 159127.
79 H. Bahreini, E. Ameri and H. Ebadi-Dehaghani, *Diamond Relat. Mater.*, 2023, **138**, 110235.
80 Y. Liu, J. Zhang and X. Tan, *ACS Omega*, 2019, **4**, 16572–16577.
81 H. Zhao, T. Song, X. Ding, R. Cai, X. Tan and Y. Zhang, *J. Membr. Sci.*, 2023, **679**, 121713.